Summary of Goldstone Orbital Debris Observations: October 1996 to May 1997

R. M. Goldstein[1]

Several times per year, on a limited basis, the Goldstone X-band (8.51-GHz) radar is used to monitor the overhead flux of orbiting debris. Data from this sensitive radar, which can detect a 3-mm fragment at a distance of 1000 km, are integrated into a debris model by a team at Johnson Space Center. The Goldstone data fill a niche in the coverage by the Haystack radar and a number of other radars, which also participate in limited observation campaigns.

In this article, we summarize the results of 10 nights of operation of the Goldstone radar, from October 1996 to May 1997. Altogether, 70 hours of data have been collected, with the radar beam aimed close to the zenith. During these times, over 2300 debris detection events were observed.

I. Introduction

Orbiting debris is recognized as a present and growing hazard for both humans and machines in space. Space collisions can have a closing velocity of 15 km s^{-1}, and even small particles are a serious safety concern. Knowledge of the changing environment of debris is necessary both for space mission design and for the assessment of debris mitigation policies.

Currently, the United States Space Command [4] maintains a catalog of orbital elements of space objects larger than about 10 cm. Monitoring of the flux of smaller objects has been accomplished by routine ground-based optical [6] and radar observations [7,8]. Very small particles of orbiting debris also have been detected in situ by spacecraft [5], which subsequently have returned to Earth. Previous results from the Goldstone radar also have been published [1–3].

II. The Radar

Two antennas were used. The transmitter, on a 70-m dish, was aimed 1.5 deg from the zenith, toward the back of the receiving antenna, a 35-m dish. The receiver was aimed 1.441 deg from the zenith, and at the same azimuth as the transmitter. Figure 1 shows the configuration. Although the two antennas are less than 500 m apart, the beams are so narrow that the area of intersection is limited to 50 km^2. This configuration permits the probing of an altitude band from about 280 to 3000 km. Signals can be detected from outside of this range, but at greatly reduced sensitivity.

[1] Telecommunications Science and Engineering Division.

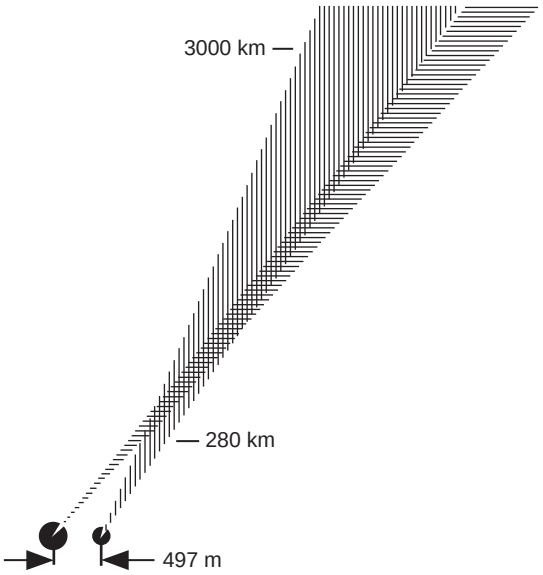

Fig. 1. Configuration of transmitting and receiving antennas, showing the region of common view.

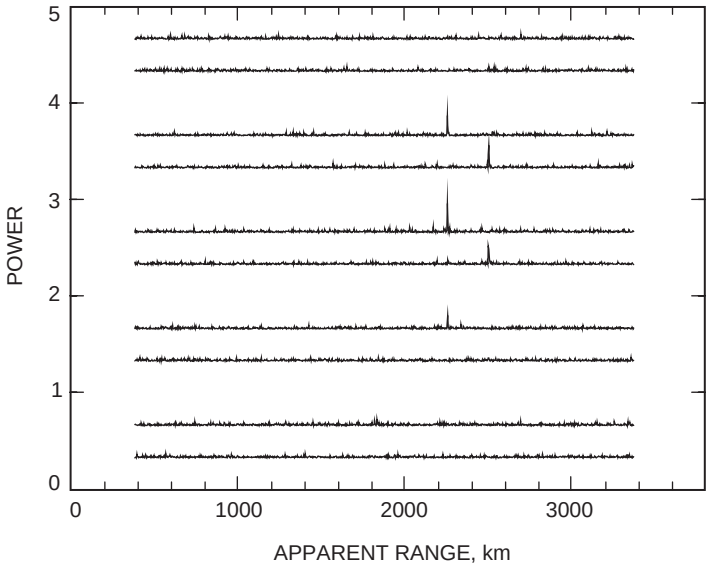

Fig. 2. System response for a typical detection of a debris particle. The results from the up-chirps are paired with those for the down-chirps. Successive pairs are spaced in time by 90 ms.

The transmitted waveform was a sequence of 46-kHz frequency chirps, each lasting 2.4 ms and followed by a listening period of 20 ms, yielding a duty cycle of 11 percent. Up-chirps were alternated with down-chirps so as to enable the separation of echo range from Doppler. Several such send–receive cycles were incoherently summed over the 90 ms or so that a particle of debris could be expected to remain in the radar beam. This cycle was repeated throughout the time available for observations.

Figure 2 shows the system result for a typical "hit." Range is the abscissa; power the ordinate. The results from the up-chirps are paired with those for the down-chirps. The pairs of responses are spaced 90 ms in time and show how the particle traversed the beam. The range can be estimated from Fig. 2 as

the average of the apparent ranges of the up- and down-chirp responses; the Doppler shift is proportional to their difference.

III. Observations

Table 1 lists the observations. Detections occurred erratically throughout the observations, from 1.2 to 2.4 minutes per hit. The average rate was 1.8 minutes per hit. Some of the events originated from strong signals in the antenna side lobes. These responses could be identified because the responses lasted for many of the nominal 90-ms beam times. They have been removed from the data set.

Table 1. Summary of observations.

Date	Hours	Hits	Power, kW	Temperature, K
10/2/96	7.5	348	495	36.1
10/8/96	5.9	297	497	35.1
11/1/96	5.4	222	495	35.8
11/24/96	7.7	275	494	34.7
12/30/96	8.7	243	360	40.1
1/31/97	10.5	284	374	42.1
3/2/97	7.9	197	370	38.8
3/26/97	8.2	260	375	33.2
4/7/97	4.4	114	370	35.8
5/18/97	3.7	112	370	36.3

IV. Results

All of the remaining data have been sorted into altitude bins of 100-km width and plotted as a histogram in Fig. 3. The peak flux of 3.5 hits per square km per day occurred at an altitude of about 900 km. Unfortunately, this flux is expected to grow steadily with time. Most, but not all, of the observed particles were in the millimetric range.

Figure 4 is a plot of effective debris size as a function of range. Effective size is defined as the size of a conducting sphere that would return the same power at the same distance as the observed object. In these calculations, the Rayleigh approximation to radar cross-section was used for particles smaller than $\lambda/4$. For larger particles, the geometric cross-section was used. The lower boundary seen in Fig. 4 is the result of the debris being below the threshold of the radar. However, for each altitude band, the flux is greatest for the smallest particles.

Figure 5 is a plot of the radial velocities as a function of range. Positive velocities indicate approaching particles. Because of the limited hardware bandwidth, debris with velocities greater than 0.8 km s^{-1} are Doppler-shifted out of the band and, hence, not detected. Near the band edge, there is a loss of sensitivity. Since the antennas are pointed slightly away from the zenith, even a circular orbit would show some radial velocity. The two major clusters in Fig. 5 likely are objects in similar orbits, with one representing ascending passes and the other descending.

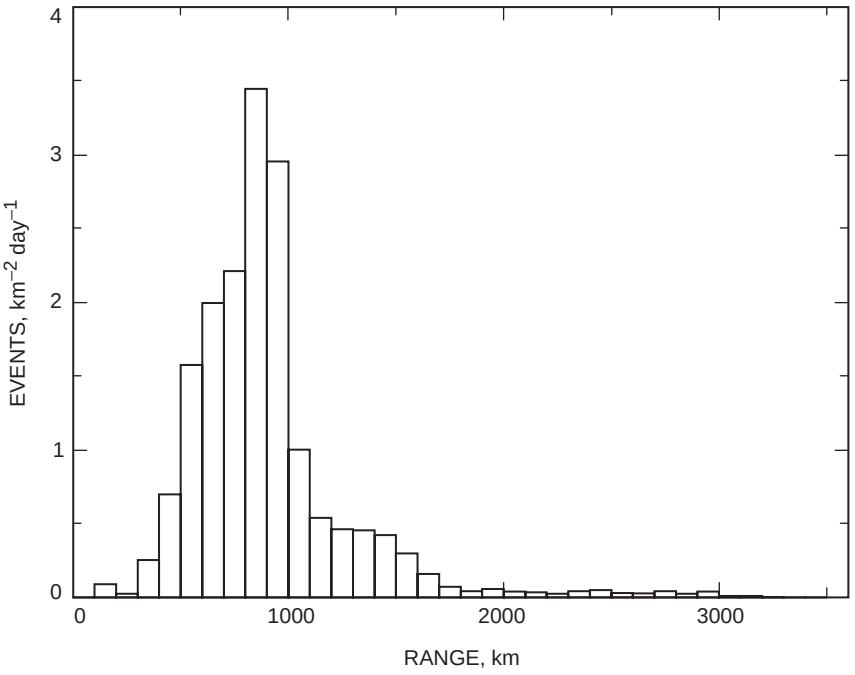

Fig. 3. Histogram of the debris flux over the 70 hours of observations.

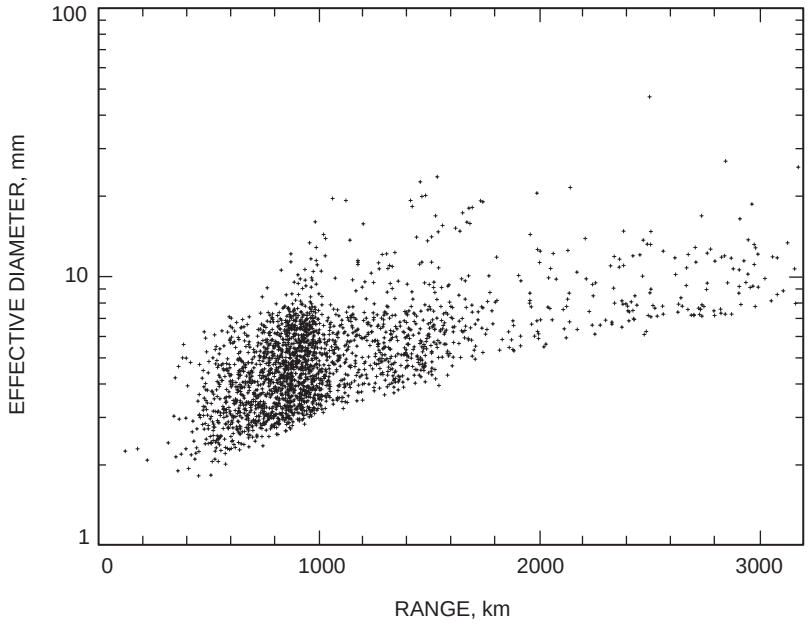

Fig. 4. Debris size as a function of range. The effective diameter is for a conducting sphere. Dielectric fragments, chips, or wires could be larger.

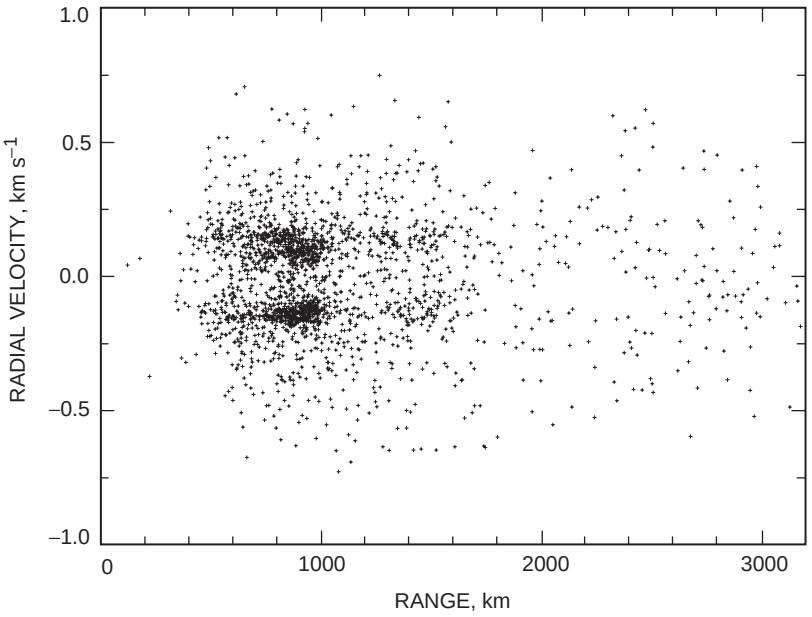

Fig. 5. Scatter plot of radial velocities versus ranges. Note the concentration of events, which suggests a common source.

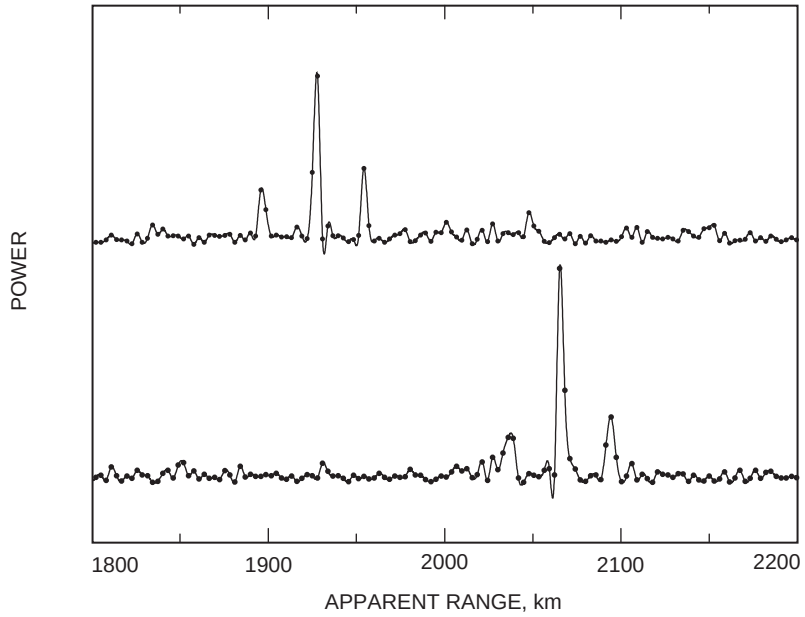

Fig. 6. Radar response to a particle that presumably is spinning rapidly.

V. Objects

Not all of the data can be classified as typical runs such as that displayed in Fig. 2. A blown-up response of one such object is given in Fig. 6, which shows significant side bands. Signal processing of the received echoes consists of convolution with the stored, transmitted chirp. When the reflected power is not constant over the duration of the chirp (perhaps the object is spinning), then the effect is Fourier transformation of the modulation. For the fragment in Fig. 6, the spinning was very rapid—3800 rev s^{-1}. Figure 7 is another example of an atypical echo. For this object, there must be some phase as well as amplitude modulation.

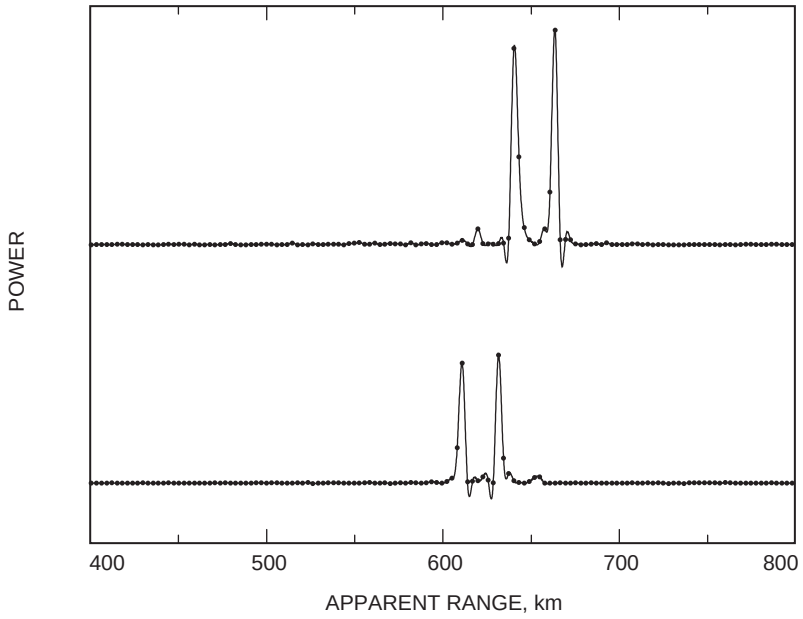

Fig. 7. Radar response to a rapidly spinning particle that produces both amplitude and phase modulation upon the echo.

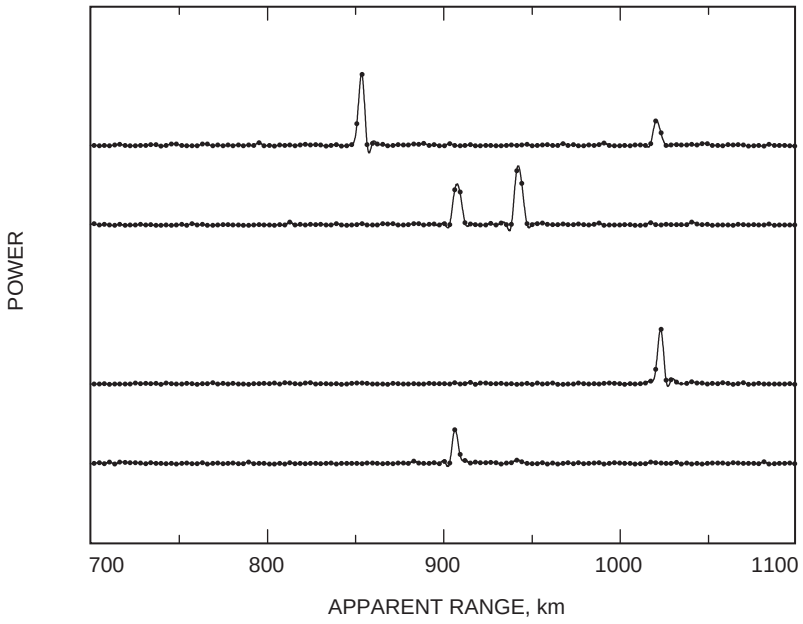

Fig. 8. Radar response when two particles are in the beam simultaneously.

The combination of up- and down-chirps permits the separate measurement of range and Doppler velocity only when there is just one reflector in the beam at a time. However, since a given fragment can remain in the beam for 90 ms, and detections occur every few minutes, there must be times when there are two objects in the beam at once. Figure 8 is an example. There are two ways to pair the echoes in the upper two traces in the figure. Fortunately, 90 ms earlier, only one of them was in the beam; thus, the ambiguity is resolved.

VI. Conclusions

Orbiting debris is a serious problem and must be addressed if the world is to continue to enjoy the use of space. The Goldstone radar is helpful in this respect; it could be more helpful with the addition of a monopulse feed at DSS 15.

References

[1] R. M. Goldstein and L. W. Randolph, "Rings of Earth, *IEEE Trans. on Microwave Theory and Techniques*, vol. 40, no. 6, pp. 1077–1080, June 1992.

[2] S. J. Goldstein and R. M. Goldstein, "Some Properties of Millimetric Space Debris," *The Astronomical Journal*, vol. 107, no. 4, pp. 367–371, January 1994.

[3] R. M. Goldstein and S. J. Goldstein, "Flux of Millimetric Space Debris," *The Astronomical Journal*, vol. 110, no. 3, pp. 1392–1396, September 1995.

[4] N. L. Johnson, "United States Space Surveillance," *Advances in Space Research*, vol. 13, no. 8, pp. 5–20, August 1993.

[5] J. C. Mandeville and L. Berthoud, "From LDEF to EURECA—Orbital Debris and Meteoroids in Low-Earth Orbits," *Advances in Space Research*, vol. 16, no. 11, pp. 67–72, 1995.

[6] A. E. Potter, "Ground-Based Optical Observations of Orbital Debris—A Review," *Advances in Space Research*, vol. 16, no. 11, pp. 35–40, 1995.

[7] E. G. Stansbery, G. Bohannon, C. Pitts, T. Tracy, and J. Stanley, "Radar Observation of Small Space Debris," *Advances in Space Research*, vol. 13, no. 8, pp. 43–48, August 1993.

[8] E. G. Stansbery, D. J. Kessler, and M. J. Matney, "Recent Results of Orbital Debris Measurements From the Haystack Radar," AIAA Paper 95-0662, 33rd Aerospace Sciences Meeting and Exhibit, Reno, Nevada, January 9–12, 1995.